X-ray absorption study of Ti-activated sodium aluminum hydride

5 AUTHORS, INCLUDING:

Jason Graetz
HRL Laboratories, LLC
106 PUBLICATIONS   2,794 CITATIONS

SEE PROFILE

J. J. Reilly
Brookhaven National Laboratory
136 PUBLICATIONS   3,646 CITATIONS

SEE PROFILE

Alex Ignatov
Rutgers, The State University of New Jersey
109 PUBLICATIONS   795 CITATIONS

SEE PROFILE

T. A. Tyson
New Jersey Institute of Technology
115 PUBLICATIONS   1,664 CITATIONS

SEE PROFILE

X-ray absorption study of Ti-activated sodium aluminum hydride

J. Graetz, J.J. Reilly, J. Johnson

Department of Energy Sciences and Technology, Brookhaven National Laboratory, Upton, New York 11973

A.Y. Ignatov, T.A. Tyson

Department of Physics, New Jersey Institute of Technology, Newark, New Jersey 07102

(Dated: February 2, 2008)

Ti K-edge x-ray absorption near edge spectroscopy (XANES) was used to explore the Ti valence and coordination in Ti-activated sodium alanate. An empirical relationship was established between the Ti valence and the Ti K-edge onset based on a set of standards. This relationship was used to estimate oxidation states of the titanium catalyst in 2 mol% and 4 mol% Ti-doped $NaAlH_4$. These results demonstrate that the formal titanium valence is zero in doped sodium alanate and nearly invariant during hydrogen cycling. A qualitative comparison of the edge fine structure suggests that the Ti is present on the surface in the form of amorphous $TiAl_3$.

There is currently considerable interest in the development of metal hydrides capable of reversible hydrogen storage at low and medium temperatures. A recent investigation of Ti-doped $NaAlH_4$ by Bogdanovic et al. has demonstrated reversible cycling in the complex metal hydrides under moderate conditions[1]. Since this discovery there has been considerable work on improving the catalytic effects and understanding the role of the catalyst in the sodium alanates. However, the mechanism by which the $NaAlH_4$ system is activated in the presence of a small amount of Ti is still not well understood. In part, this is because the location and valence of the activating species is unknown.

In sodium aluminum hydride, the hydrogen absorption/desorption occurs through the following two-step decomposition-recombination reaction:

$$NaAlH_4 \leftrightarrow \frac{1}{3}Na_3AlH_6 + \frac{2}{3}Al + H_2 \leftrightarrow NaH + Al + \frac{3}{2}H_2 \quad (1)$$
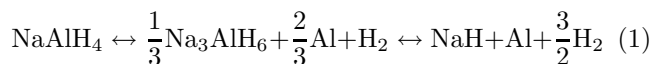
giving a combined theoretical hydrogen storage capacity of 5.6 wt%. There are a number of possible mechanisms by which a metal dopant might enhance the dehydriding kinetics of equation 1[2]. The simplest possibility is that the Ti acts as a classic catalyst and assists the conversion of atomic hydrogen into molecular hydrogen at the surface. This situation is unlikely due to the strong thermodynamic driving force on the Ti to form a hydride in the presence of the desorbed hydrogen.

Another proposed mechanism for the activation of $NaAlH_4$ involves the substitution of the dopant into the lattice. A recent x-ray diffraction study of Ti and Zr-doped $NaAlH_4$ has demonstrated lattice distortions associated with doping the hydride[10]. Based on these distortions, Sun et al. have suggested that the Ti is substituted for the Na cation[7,10] and is present as Ti^{4+} at doping levels $\leq$ 2 mol%. The enhanced kinetics are attributed to vacancy formation and the lattice distortion associated with the bulk lattice substitution.

A final possibility is that the hydrogen diffuses to the surface in an Al-H complex where it is dissociated by the catalyzing agent and releases H_2. This process leads to a significant coalescence of Al on the particle surface in the dehydrided state. Energy dispersive spectroscopy of Ti-doped $NaAlH_4$ has revealed Al segregation towards regions of higher Ti concentration on the particle surface upon the initial dehydrogenation[4]. The presence of zero-valent Ti is also supported by H_2 evolution during the

doping process[1,3]. Other investigations of Ti-activated sodium alanate have demonstrated the formation of a $TiAl_3$ phase upon ball milling a 3:1 mixture of $NaAlH_4$ and $TiCl_3$[5]. However, it has been shown that only 2 % of the metal is required to activate $NaAlH_4$[7,8,9]. Therefore, studies of excessively-doped $NaAlH_4$ yield properties of the excess metal and not the activating species.

This letter presents XAS measurements of the Ti K-edge from the 2 mol% and 4 mol% Ti-doped $NaAlH_4$. The Ti valence was determined using the x-ray absorption near-edge structure.

Ti-doped $NaAlH_4$ was prepared by mechanically milling 95% pure $NaAlH_4$ (Alfa) with $TiCl_3$ (Aldrich 99%) in a Fritsch Pulverisette 6 planetary mill. The powders ($\sim$ 1.2 g) were milled in a 250 mL tungsten carbide bowl using seven 15 mm diameter WC balls ($\sim$ 26 g each). The mechanical attrition was performed in an inert Ar atmosphere for 1.5 hours. Samples containing 2 mol% and 4 mol% $TiCl_3$ were prepared for this study. The Ti-doped materials were hydrided/dehydrided in a calibrated fixed-volume for 4 cycles to ensure a homogenous Ti distribution. $TiH_{1.1}$ was prepared by dehydriding TiH_2 (Alfa 99%) at 700° C into a calibrated fixed volume. $TiAl_3$, $Ti_{0.08}Al_{0.92}$ and $Ti_{0.02}Al_{0.98}$ were prepared by arc melting the components in a He atmosphere. The FeTi and $TiAl_3$ were crushed into a powder, while the more ductile alloys of $Ti_{0.08}Al_{0.92}$ and $Ti_{0.02}Al_{0.98}$ were pressed into a thin pellet (123 MPa). Other Ti-containing materials included powders of TiO (Alfa 99.5 %), Ti_2O_3 (Aldrich 99.9%), TiO_2 (Johnson Matthey 99.995%), FeTi (Canon-Muskegon 99%), $TiCl_3$ (Aldrich 99.999%) and TiH_2 (Alfa 99%), and a foil of Ti metal (Materials Research Corp. 99.97%). All powders were sieved through a 325 mesh (44 μm) and brushed onto Kapton tape.

Ti K-edge spectra were collected at beamline X-19A at the National Synchrotron Radiation Light Source (NSLS) using a Si(111) double crystal monochromator. The higher-order harmonics were suppressed by detuning the second crystal of the monochromator on its rocking curve to 50 % of the maximum transmitted intensity at 400 eV above the edge. Spectra were recorded in fluorescence yield using a PIPS detector for the reasonably concentrated samples and a 13-element Ge detector (Canberra) with an energy resolution of 240 eV for the diluted samples. All samples were kept at room temperature and oriented to have the incident x-ray striking the surface at 45 ± 5°. This geometry provided essentially bulk-sensitive measurements. Due to small Ti con-
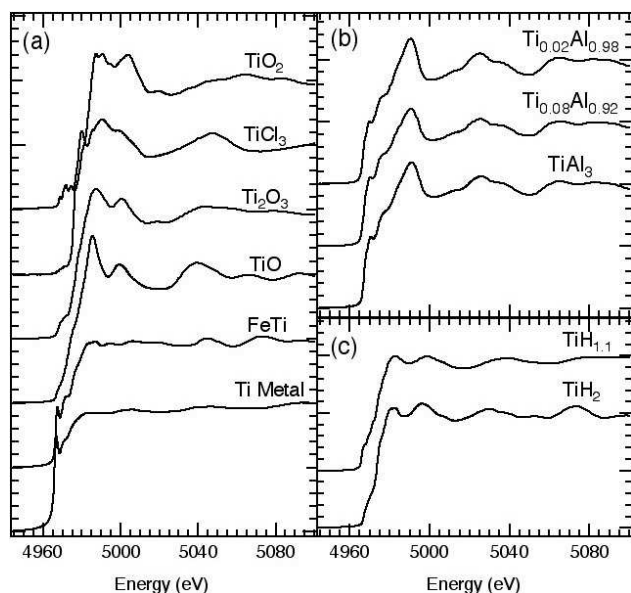
FIG. 1: (**a**) Ti K-edges from Ti metal, FeTi, TiO, Ti_2O_3, $TiCl_3$, TiO_2, (**b**) $TiAl_3$, nonstoichiometric $Ti_{0.08}Al_{0.92}$ and $Ti_{0.02}Al_{0.98}$, (**c**) TiH_2 and nonstoichiometric $TiH_{1.14}$.

FIG. 2: Shift in the Ti K-edge onset energy with respect to the formal oxidation state in a series of Ti standards.

centrations, the XANES spectra were not corrected for "self-absorption". The energy scale was calibrated by assigning $E = 4966$ eV to the first inflection point of the pure Ti foil with an error of less than 0.1 eV. Air sensitive samples were measured in a sealed sample holder after being loaded in a glove box under Ar. All spectra were background subtracted and normalized to a 100 eV window, 100 eV above the edge onset.

Powder x-ray diffraction (Rigaku Miniflex) of the Ti-doped $NaAlH_4$ after mechanical attrition revealed the presence of $NaAlH_4$ with some minor concentrations of αNa_3AlH_6, metallic Al, and NaCl. A small amount of NaCl is initially formed upon ball milling, which results in the decomposition of a small amount of $NaAlH_4$. X-ray diffraction of the cycled samples suggests that additional NaCl (and Al metal) is formed upon cycling. The majority species in both dehydrided samples were NaH and metallic aluminum, consistent with equation 1. The hydrided 2 mol% Ti sample consisted of predominately $NaAlH_4$, while the 4 mol% Ti material exhibited more of a mixed phase, with $NaAlH_4$ and minor concentrations of αNa_3AlH_6 and metallic Al, suggesting the hydrogenation did not go to completion in this sample.

The Ti K-edges from a series of Ti standards are displayed in Fig. 1a. The Ti edges for $TiAl_3$ and two Al samples with 2 mol% and 8 mol% Ti are shown in Fig. 1b. The edges from the three different Ti concentrations are qualitatively identical. This is not surprising, since Ti is immiscible in Al at room temperature and will nucleate the $TiAl_3$ phase even at low dopant levels[12]. The Ti K-edges from TiH_2 and $TiH_{1.1}$ (Fig. 1c) are also very similar, indicating that the structural environment around the Ti is essentially the same. However, the local disorder in the substoichiometric compound ($TiH_{1.1}$) is clearly visible above the edge.

The most interesting features of Fig. 1 are the large chemical shifts in the Ti K-edge, relative to Ti metal. The shift of the Ti K-edge reflects changes in the binding
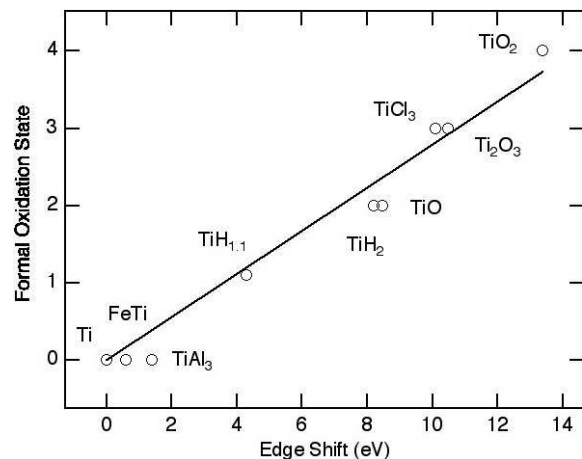
energy of the Ti $1s$ electron. The largest observed shift is about 13 eV between Ti metal, containing neutral Ti atoms, and TiO_2, containing Ti^{4+}. The increase in the $1s$ binding energy is due to the reduced screening of the nuclear charge as the outer electrons are pulled off the atom.

A plot of the relationship between the edge onset and the Ti valence is shown in Fig. 2. The onset of the K-edge was defined by the maximum of the first derivative. In cases where the peak in the first derivative was clearly split, such as $TiH_{1.1}$, the onset was chosen as the midpoint between the two peaks. There is a linear correlation between the oxidation state of the Ti ion, n, and the edge shift with respect to Ti metal, ΔE. This relationship ($n = x\Delta E$) has a coefficient of $x = 0.28 \pm 0.01$.

The edge onset energies were used to determine the Ti valence in the Ti-doped sodium alanates and the results are displayed in Table I. In the hydrided and dehydrided compounds the Ti is essentially zero-valent (total charge transfer of half an electron, or less). Although the neutral
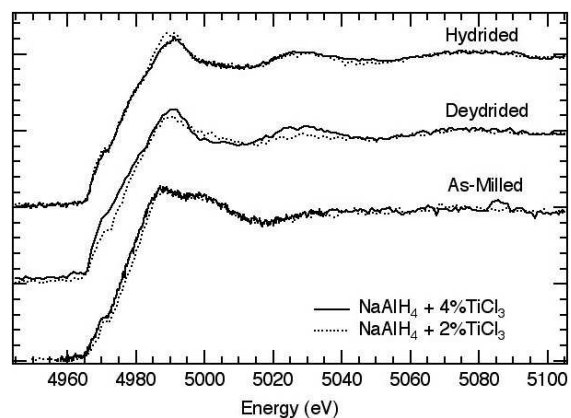

FIG. 3: Ti K-edges from sodium alanate doped with 2 mol% (thin line) and 4 mol% Ti (thick line). Edges are shown for the mechanically-milled material (no cycling), the dehydrided and the hydrided material after four cycles.

TABLE I: Measured Ti K-edge onset energies and corresponding oxidation states for the Ti-doped sodium alanates

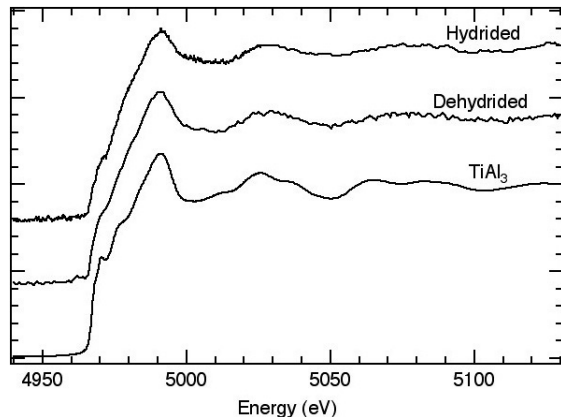| Dopant	Condition	Edge Shift (eV)	Oxidation State
4 mol% Ti	dehydrided	0.6	0.17 ± 0.01
4 mol% Ti	hydrided	1.3	0.36 ± 0.01
2 mol% Ti	dehydrided	1.9	0.53 ± 0.02
2 mol% Ti	hydrided	1.9	0.53 ± 0.02

FIG. 4: Ti K-edges from $TiAl_3$ and 2 mol% Ti-doped sodium alanate in the hydrided and dehydrided states.

character of the Ti valence is supported by a number of other studies[1,3,4,5,6], this is the first direct evidence of zero-valent Ti at dopant levels of 2–4 mol%. The Ti K-edge from the as-milled material is believed to be a superposition of edges and therefore, no oxidation states were calculated.

The structure of the Ti K-edge can also be used to gain insight into the local Ti environment. Figure 4 displays a plot of the Ti K-edge from the hydrided and dehydrided 2 mol% Ti-doped sodium alanates and $TiAl_3$. In the doped sodium alanates, a small shoulder is evident just above the main peak (4998–5010 eV), which may be attributed to the presence of a small amount of near-by hydrogen.

The formation of titanium hydride is not unlikely since the presence of any Ti metal would likely form TiH_{2-x} during the first desorption. Despite this minor difference, the fine structure above the edge (4960–5100 eV) is qualitatively similar for the Ti-activated alanates and $TiAl_3$. This suggests that the Ti is coordinated by Al atoms and that the local order is similar to that of $TiAl_3$. This is not surprising since $TiAl_3$ is the most thermodynamically favorable Ti product ($\Delta H_{298K} = -142.4$ kJ/mol[13]), followed by TiH_2 ($\Delta H_{298K} = -119.7$ kJ/mol[14]) and Ti_3Al ($\Delta H_{298K} = -100.5$ kJ/mol[13]). However, the oscillations are clearly less pronounced in the doped alanates, suggesting that the Ti lacks the long range order that exists in crystalline $TiAl_3$. This supports the recent study of Weidenthaler et al. that demonstrated that Ti is atomically dispersed and essentially amorphous in this system[15]. The lack of long-range order would also explain why $TiAl_3$ has never been directly observed at these dopant levels through diffraction techniques.

The Ti K-edge of the mechanically milled material (no cycling) exhibits peaks at 4988 eV 4998 eV (Fig. 3). This structure may be indicative of a superposition of edges from Ti in multiple environments, the initial $TiCl_3$, TiH_{2-x}, and possibly $TiAl_3$. The decomposition of $NaAlH_4$ during mechanical milling liberates Al and H_2, either of which may form a compound with Ti. Although $TiAl_3$ is more stable, the liberated H_2 is considerably more mobile and therefore more likely to react with Ti, forming TiH_{2-x}. It is likely that the formation of $TiAl_3$ predominately occurs during the first decomposition, where metallic Al is more abundant.

A final interesting feature of Fig. 3 is the similarity of the hydrided and dehydrided spectra. This suggests that the local environment around the Ti is nearly invariant during the hydrogen cycle (equation 1). Although there is no long-range order, the Ti is locally coordinated by Al at every stage of the reaction.

These results confirm that the Ti is not present in the form of Ti metal and clearly demonstrate that there is no bulk lattice substitution. The catalyzing agent in Ti-doped $NaAlH_4$ is present on the surface in the form of amorphous $TiAl_3$.

[1] B. Bogdanovic and M. Schwickardi. *J. Alloys Comp.*, 253–254:1–9, 1997.

[2] K. J. Gross, S. Guthrie, S. Takara, and G. Thomas. *J. Alloys Comp.*, 297:270–281, 2000.

[3] B. Bogdanovic, R. Brand, Marjanovic A., Schwickardi M., and Tolle J. *J. Alloys Comp.*, 302:36–58, 2000.

[4] G. J. Thomas, K. J. Gross, N. Y. C. Yang, and C. Jensen. *J. Alloys Comp.*, 330–332:702–707, 2002.

[5] E. H. Majzoub and K. J. Gross. *J. Alloys Comp.*, 356–357:363–367, 2003.

[6] V. P. Balema, J. W. Wiench, K. W. Dennis, M. Pruski, and Pecharsky V. K. *J. Alloys Comp.*, 329:108–114, 2001.

[7] C. M. Jensen and R. Zidan. *Int. J. Hydrogen Energy*, 24:461–465, 1999.

[8] G. Sandrock, K. J. Gross, G. Thomas, C. Jensen, D. Meeker, and S. Takara. *J. Alloys Comp.*, 330–332:696–701, 2002.

[9] R. A. Zidan, S. Takara, A. G. Hee, and C. M. Jensen. *J. Alloys Comp.*, 285:119–112, 1999.

[10] D. Sun, T. Kiyobayashi, H. T. Takeshita, N. Kuriyama, and C. M. Jensen. *J. Alloys Comp.*, 337:L8–L11, 2002.

[11] K. J. Gross, E. H. Majzoub, and S. W. Spangler. *J. Alloys Comp.*, 356–356:423–428, 2003.

[12] R. D. Massalski, editor. *Binary Alloy Phase Diagrams, V.1.* ASM International, 1990.

[13] C. J. Smithells. *Metals Reference Book, 4th ed.* Butterworth & Co., London, 1967.

[14] *Handbook of Chemistry and Physics, 64th ed.* CRC Press, Boca Raton, 1983.

[15] C. Weidenthaler, A. Pommerin, M. Felderhoff, B. Bogdanovic, and F. Schuth. *Phys. Chem. Chem. Phys.*, 5:5149–5153, 2003.